Inorg. Chem. **2005**, *44*, 6670–6679

Nitrosylated Iron–Thiolate–Sulfinate Complexes with $\{Fe(NO)\}^{6/7}$ Electronic Cores: Relevance to the Transformation between the Active and Inactive NO-Bound Forms of Iron-Containing Nitrile Hydratases

Chien-Ming Lee,[†] Chien-Hong Chen,[†] Hao-Wen Chen,[†,‡] Jo-Lu Hsu,[†,‡] Gene-Hsiang Lee,[§] and Wen-Feng Liaw*[,†]

Department of Chemistry, National Tsing Hua University, Hsinchu 30013, Taiwan, Department of Chemistry, National Changhua University of Education, Changhua, Taiwan, and Instrumentation Center, National Taiwan University, Taipei, Taiwan

Received January 24, 2005

The five-coordinated iron–thiolate nitrosyl complexes $[(NO)Fe(S,S\text{-}C_6H_3R)_2]^-$ (R = H (**1**), *m*-CH_3 (**2**)), $[(NO)Fe(S,S\text{-}C_6H_2\text{-}3,6\text{-}Cl_2)_2]^-$ (**3**), $[(NO)Fe(S,S\text{-}C_6H_3R)_2]^{2-}$ (R = H (**10**), *m*-CH_3 (**11**)), and $[(NO)Fe(S,S\text{-}C_6H_2\text{-}3,6\text{-}Cl_2)_2]^{2-}$ (**12**) have been isolated and structurally characterized. Sulfur oxygenation of iron–thiolate nitrosyl complexes **1**–**3** containing the $\{Fe(NO)\}^6$ core was triggered by O_2 to yield the S-bonded monosulfinate iron species $[(NO)Fe(S,SO_2\text{-}C_6H_3R)(S,S\text{-}C_6H_3R)]^-$ (R = H (**4**), *m*-CH_3 (**5**)) and $[(NO)Fe(S,SO_2\text{-}C_6H_2\text{-}3,6\text{-}Cl_2)(S,S\text{-}C_6H_2\text{-}3,6\text{-}Cl_2)]_2^{2-}$ (**6**), respectively. In contrast, attack of O_2 on the $\{Fe(NO)\}^7$ complex **10** led to the formation of complex **1** accompanied by the minor products, $[Fe(S,S\text{-}C_6H_4)_2]_2^{2-}$ and $[NO_3]^-$ (yield 9%). Reduction of complexes **4**–**6** by $[EtS]^-$ in CH_3CN–THF yielded $[(NO)Fe(S,SO_2\text{-}C_6H_3R)(S,S\text{-}C_6H_3R)]^{2-}$ (R = H (**7**), *m*-CH_3 (**8**)) and $[(NO)Fe(S,SO_2\text{-}C_6H_2\text{-}3,6\text{-}Cl_2)(S,S\text{-}C_6H_2\text{-}3,6\text{-}Cl_2)]^{2-}$ (**9**) along with $(EtS)_2$ identified by ^1H NMR. Compared to complex **10**, complexes **7**–**9** with the less electron-donating sulfinate ligand coordinated to the $\{Fe(NO)\}^7$ core were oxidized by O_2 to yield complexes **4**–**6**. Obviously, the electronic perturbation of the $\{Fe(NO)\}^7$ core caused by the coordinated sulfinate in complexes **7**–**9** may serve to regulate the reactivity of complexes **7**–**9** toward O_2. The iron–sulfinate nitrosyl species with the $\{Fe(NO)\}^{6/7}$ core exhibit the photolabilization of sulfur-bound [O] moiety. Complexes **1**–**4**–**7**–**10** (or **2**–**5**–**8**–**11** and **3**–**6**–**9**–**12**) are interconvertible under sulfur oxygenation, redox processes, and photolysis, respectively.

Introduction

Mononuclear non-heme iron centers are present in the catalytic cycle of a number of proteins involved in oxygen activation.[1,2] Nitrile hydratase (NHase) is a metalloenzyme which catalyzes the hydrolysis of nitriles to the corresponding amides.[3,4] Crystallographic studies have shown that the active-site structure of the Fe-NHase (Fe-containing nitrile hydratase) active form isolated from *Brevibacterium* R312 consists of a paramagnetic, low-spin Fe(III) center coordinated by two deprotonated carboxamido nitrogens from the peptide backbone, three facial cysteine sulfurs, and a water or hydroxide molecule.[5] The X-ray crystallographic studies on the inactive form of the Fe-NHase from *Rhodococcus* sp. N-771 (and *Rhodococcus* sp. R312) revealed that the iron center is coordinated by two deprotonated carboxamido nitrogens, three Cys-S residues with two of them posttranslationally modified to Cys-sulfinic (Cys-SO_2) and Cys-sulfenic (Cys-SO) groups, and a NO molecule.[6] Such modified cysteines residues (sulfinate RSO_2^- and sulfenate RSO^- groups) are unprecedented.[3−6] An inactive, NO-bound

* To whom correspondence should be addressed. E-mail: wfliaw@mx.nthu.edu.tw.
† National Tsing Hua University.
‡ National Changhua University of Education.
§ National Taiwan University.

(1) Feig, A. L.; Lippard, S. J. *Chem. Rev.* **1994**, *94*, 759.
(2) Solomon, E. I.; Zhang, Y. *Acc. Chem. Res.* **1992**, *25*, 343.
(3) (a) Kobayashi, M.; Shimizu, S. *Nat. Biotechnol.* **1998**, *16*, 733. (b) Kobayashi, M.; Nagasawa, T.; Yamada, H. *Trends Biotechnol.* **1992**, *10*, 402.
(4) (a) Brennan, B. A.; Alms, G.; Nelson, M. J.; Durney, L. T.; Scarrow, R. C. *J. Am. Chem. Soc.* **1996**, *118*, 9194. (b) Sugiura, Y.; Kuwahara, J.; Nagasawa, T.; Yamada, H. *J. Am. Chem. Soc.* **1987**, *109*, 5848.
(5) Huang, W.; Jia, J.; Cummings, J.; Nelson, M.; Schneider, G.; Lindqvist, Y. *Structure* **1997**, *5*, 691.
(6) (a) Nagashima, S.; Nakasako, M.; Dohmae, N.; Tsujimura, M.; Takio, K.; Odaka, M.; Yohda, M.; Kamiya, N.; Endo, I. *Nat. Struct. Biol.* **1998**, *5*, 347. (b) Scarrow, R. C.; Stickler, B. S.; Ellison, J. J.; Shoner, S. C.; Kovacs, J. A.; Cummings, J. C.; Nelson, M. J. *J. Am. Chem. Soc.* **1998**, *120*, 9237.

10.1021/ic050108l CCC: $30.25
Published on Web 08/16/2005

form is generated in cells grown in the dark, and the active form of the Fe-NHase is regenerated with release of NO molecule upon exposure to light.[7,8] Interestingly, recent studies demonstrated that atmospheric oxygen activates the reconstituted nitrile hydratase through specific modifications of Cys112 and Cys114 to Cys-SO_2H and Cys-SOH, respectively, and Cys112-SO_2H is responsible for the catalytic activity solely or in combination with Cys114-SOH.[9] The role/function of the NO ligand, NO binding to the iron active site before or after Cys-S oxygenation, the oxidant(s) responsible for the posttranslational modifications of the bound Cys-S donors at the active site of the enzyme, the function and biogenic mechanism of these modified cysteine-sulfinic and -sulfenic groups, and the reason(s) for the asymmetric oxygenation of the two Cys-S ligands are the principal questions to be raised in the chemistry of Fe-NHase.[10−12]

Some iron−thiolate nitrosyl model compounds have been reported recently by Kovacs et al.,[10] Mascharak et al.,[11a,b] and Artaud et al.,[11c] respectively. In one interesting model compound the diamagnetic Fe(III)−nitrosyl complex $[FeS_2^{Me2}N_3(Pr,Pr)(NO)]^+$ ($S_2^{Me2}N_3(Pr,Pr)$ = 3-methyl-3-mercapto-2-butanone) with the $\{Fe(NO)\}^6$ core, obtained from reaction of the paramagnetic $[FeS_2^{Me2}N_3(Pr,Pr)]^+$ and NO, displayed antiferromagnetic coupling between d^5 Fe^{III} and •NO.[10] The S-bonded sulfinato iron(III) complexes $[Fe(PyPepSO_2)_2]^-$ was obtained from sulfur oxygenation of $[Fe(PyPepS)_2]^-$ ($PyPepSH_2$ = *N*-2-mercaptophenyl-2′-pyridinecarnoxamide) by H_2O_2.[11a−b] In a recent communication, we have shown that the iron−nitrosyl complex containing S-bonded monosulfinate $[(NO)Fe(S,SO_2\text{-}C_6H_4)(S,S\text{-}C_6H_4)]^-$ (**4**) was isolated from sulfur oxygenation of complex $[(NO)Fe(S,S\text{-}C_6H_4)_2]^-$ (**1**) (Scheme 1a).[13] This result reveals that binding of NO to the iron center promotes sulfur oxygenation by dioxygen and stabilizes the S-bonded sulfinate iron species. Reaction of complex **4** and excess PPh_3 yielded complex **1** and Ph_3PO (Scheme 1a′).[13] Alternatively, upon photolysis of CH_2Cl_2 solution of complex **4** under N_2 purge at ambient temperature, the UV−vis and IR spectra consistent with the formation of complex **1** demonstrate that complexes **1** and **4** are photochemically interconvertible.[13]

Scheme 1

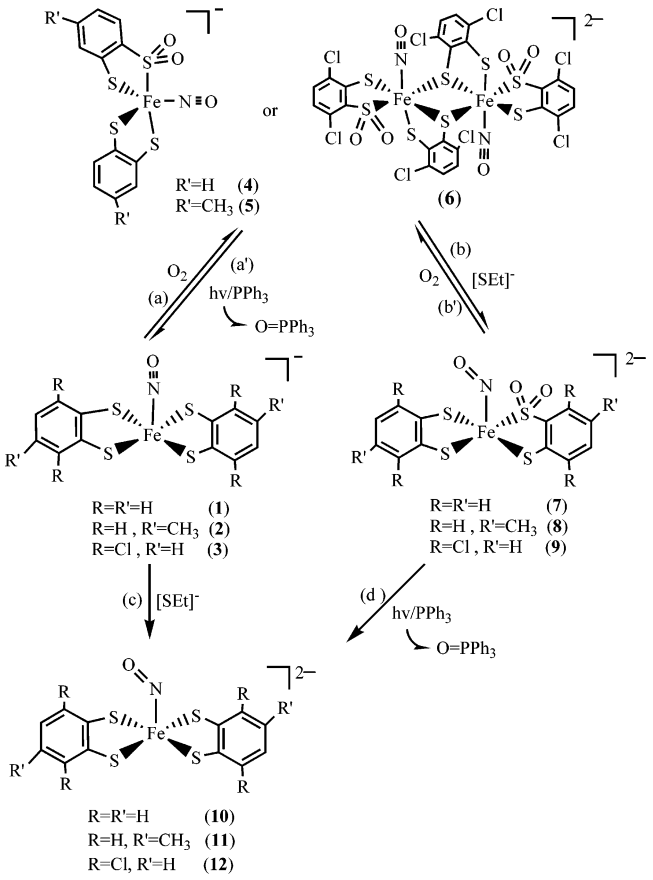

In this paper, studies of the reactivity of the $\{Fe(NO)\}^n$ (n = 6, 7) iron−thiolate and iron−sulfinate nitrosyl complexes toward O_2, the influence of sulfinate ligand on Fe−N−O bonding and on the electronic structure of the $\{Fe(NO)\}^{6/7}$ core, and the photochemical interconversion between iron−thiolate and iron−sulfinate−thiolate nitrosyl complexes may provide valuable insights into the interconversion pathways between the active and inactive NO-bound forms of Fe-containing nitrile hydratase. Here, the formalism $\{M(NO)_x\}^y$ (where y = the number of d-type electrons and is the conventional number of d-electrons for the metal center when the NO ligand is considered to be NO^+) invokes the Enemark−Feltham notation, which stresses the well-known covalency and delocalization in the electronically amorphous $M(NO)_x$ unit, i.e., without committing to a formal oxidation state on M and NO.[14] In addition, this study also details the effect of S-atom electron density on the sulfur oxygenation of the similar iron−thiolate−nitrosyl compounds, and the reactivity of the iron−sulfinate nitrosyl complexes toward O_2 is compared with that of the iron−thiolate analogues.

Results and Discussion

Sulfur Oxygenation of the $\{Fe(NO)\}^6$ Complexes. As presented in Scheme 1a, the $\{Fe(NO)\}^6$ $[(NO)Fe(S,S\text{-}C_6H_3R)_2]^-$ (R = H (**1**), *m*-CH_3 (**2**)) complexes reacted slowly with molecular oxygen in CH_2Cl_2 solution at room temperature to yield the corresponding S-bonded monosulfinate

(7) Noguchi, T.; Hoshino, M.; Tsujimura, M.; Odaka, M.; Inoue, Y.; Endo, I. *Biochemistry* **1996**, *35*, 16777.
(8) Odaka, M.; Fujii, K.; Hoshino, M.; Noguchi, T.; Tsujimura, M.; Nagashima, S.; Yohda, M.; Nagamune, T.; Inoue, Y.; Endo, I. *J. Am. Chem. Soc*. **1997**, *119*, 3785.
(9) Murakami, T.; Nojiri, M.; Nakayama, H.; Odaka, M.; Yohda, M.; Dohmae, N.; Takio, K.; Nagamune, T.; Endo, I. *Protein Sci.* **2000**, *9*, 1024.
(10) (a) Schweitzer, D.; Ellison, J. J.; Shoner, S. C.; Lovell, S.; Kovacs, J. A. *J. Am. Chem. Soc*. **1998**, *120*, 10996. (b) Shearer, J.; Jackson, H. L.; Schweitzer, D.; Rittenberg, D. K.; Leavy, T. M.; Kaminsky, W.; Scarrow, R. C.; Kovacs, J. A. *J. Am. Chem. Soc*. **2002**, *124*, 11417.
(11) (a) Tyler, L. A.; Noveron, J. C.; Olmstead, M. M.; Mascharak, P. K. *Inorg. Chem*. **1999**, *38*, 616. (b) Noveron, J. C.; Olmstead, M. M.; Mascharak, P. K. *J. Am. Chem. Soc*. **2001**, *123*, 3247. (c) Artaud, I.; Chatel, S.; Chauvin, A. S.; Bonnet, D.; Kopf, M. A.; Leduc, P. *Coord. Chem. Rev*. **1999**, *190-192*, 577. (d) Mascharak, P. K. *Coord. Chem. Rev*. **2002**, *225*, 201.
(12) Noguchi, T.; Honda, J.; Nagamune, T.; Sasabe, H.; Inoue, Y.; Endo, I. *FEBS Lett.* **1995**, *358*, 9.
(13) Lee, C.-M.; Hsieh, C.-H.; Dutta, A.; Lee, G.-H.; Liaw, W.-F. *J. Am. Chem. Soc*. **2003**, *125*, 11492.
(14) Enemark, J. H.; Feltham, R. D. *Coord. Chem. Rev*. **1974**, *13*, 339.

iron−nitrosyl complexes $[(NO)Fe(S,SO_2\text{-}C_6H_3R)(S,S\text{-}C_6H_3R)]^-$ (R = H (**4**), *m*-CH_3 (**5**)) in which the bound thiolato sulfur is oxygenated to the sulfinato group.[13,15,16] The dark purple solids **4** and **5** were isolated in 21% and 20% yield after the mixture solution was separated by silica gel chromatography with THF and CH_2Cl_2 as eluant and recrystallized with THF (or CH_3CN) and diethyl ether, respectively.

Upon injection of O_2 gas into a CH_2Cl_2 solution of complex $[(NO)Fe(S,S\text{-}C_6H_2\text{-}3,6\text{-}Cl_2)_2]^-$ (**3**), a reaction ensued over the course of 1 week to give the dimeric $[(NO)Fe(S,SO_2\text{-}C_6H_2\text{-}3,6\text{-}Cl_2)(S,S\text{-}C_6H_2\text{-}3,6\text{-}Cl_2)]_2^{2-}$ (**6**) identified by X-ray crystal structure. In complex **6**, the sixth site of each iron is ligated to one of the bound thiolato sulfurs of the other $[(NO)Fe(S,SO_2\text{-}C_6H_2\text{-}3,6\text{-}Cl_2)(S,S\text{-}C_6H_2\text{-}3,6\text{-}Cl_2)]^-$ moiety (Scheme 1a). The infrared spectrum of complex **6** showing strong bands at 1844, 1801 and 1217 m, 1083 m cm^{-1} (KBr) corresponding to the ν(NO) and ν(SO) stretching frequencies of the S-bonded sulfinate group, respectively. Formation of complex **6** can be interpreted as coordinative association of two monoanionic $[(NO)Fe(S,SO_2\text{-}C_6H_2\text{-}3,6\text{-}Cl_2)(S,S\text{-}C_6H_2\text{-}3,6\text{-}Cl_2)]^-$. It may be attributed to the electron deficiency at the iron center, derived from the existence of one sulfinate group. In complexes **1**−**3**, NO bound to an iron center leading to an $\{Fe(NO)\}^6$ system triggers sulfur oxygenation to yield iron−sulfinate nitrosyl complexes **4**−**6**. To prove that the bound NO is responsible for sulfur oxygenation, we repeated the reaction of $[Fe(S,S\text{-}C_6H_4)_2]_2^{2-}$ and $[(C_4H_8O)Fe(S,S\text{-}C_6H_4)_2]^-$ with dioxygen in THF, respectively. On the basis of IR ν(SO) spectra for both of the solution sample and the insoluble solid sample, no iron−sulfinate compounds were generated after the reaction solution was stirred in THF/CH_2Cl_2 for 6 days; instead, an insoluble yellow solid occurred. The insoluble solid (in CH_3CN/CH_3OH) has not been characterized at this time. However, we cannot unambiguously rule out the possibility of formation of sulfinate/sulfenate species instead of iron−sulfinate complexes.

O-atom transfer has been observed in the presence of PPh_3 from the sulfenate group in the Ni complex.[17] Conversion of complex **6** to **3** was displayed when CH_2Cl_2 solution (3 mL) of complex **6** (0.1 mM) and PPh_3 (1 mM) was photolyzed under N_2 purge at ambient temperature for 20 min (Scheme 1a′); the shift in electronic absorptions at 528 and 974 nm to 500 and 1248 nm is accompanied by a color change from purple to dark reddish brown which is in accord with the formation of complex **3**.

The magnetic measurements and the ^{1}H NMR spectra confirm complexes **1**−**3** are diamagnetic species.[13] Also, diamagnetism of complexes **4**−**6** is confirmed by the EPR silence, the ^{1}H NMR spectra, and the magnetic measurements. As can be inferred from the reported data,[18−20] the

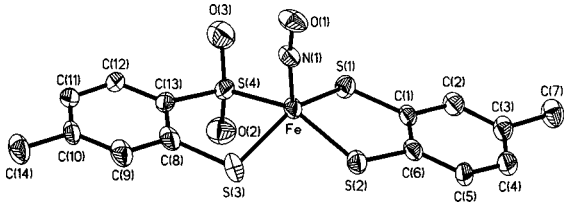

Figure 1. ORTEP drawing and labeling scheme of complex **5**. Selected bonds (Å): Fe−N(1), 1.622(5); Fe−S(1), 2.2019(18); Fe−S(2), 2.1817(18); Fe−S(3), 2.282(2); Fe−S(4), 2.2345(18); N(1)−O(1), 1.162(6); S(4)−O(2), 1.425(5); S(4)−O(3), 1.385(6). Selected angles (deg): Fe−N(1)−O(1), 171.9(5); S(1)−Fe−S(3), 150.45(8); S(2)−Fe−S(4), 152.25(7); S(2)−Fe−S(1), 88.94(6); S(3)−Fe−S(4), 85.51(7); N(1)−Fe−S(1), 109.39(18); N(1)−Fe−S(2), 105.9(2); N(1)−Fe−S(3), 100.02(18); N(1)−Fe−S(4), 101.53(19).

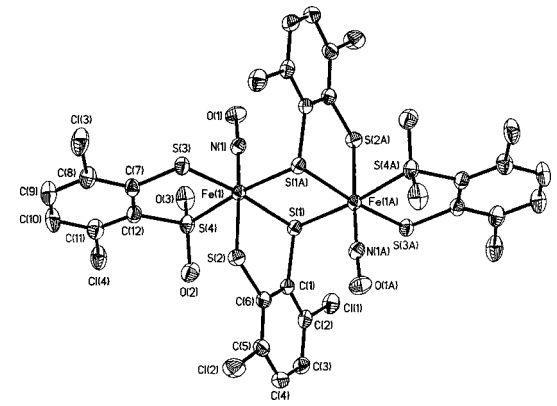

Figure 2. ORTEP drawing and labeling scheme of complex **6**. Selected bonds (Å): Fe(1)−N(1), 1.651(2); Fe(1)−S(1), 2.2986(8); Fe(1)−S(3), 2.2941(8); Fe(1)−S(2), 2.2829(8); Fe(1)−S(4), 2.2506(9); N(1)−O(1), 1.154(3). Selected angle (deg): Fe−N(1)−O(1), 177.1(2).

UV−vis spectra of complexes **4**−**6** exhibit an intense absorption around 980 nm with extinction coefficient $\epsilon >$ 4000 L mol^{-1} cm^{-1} which is ascribed to the intervalence transition M(L)(L•) ↔ M(L•)(L) (L = 1,2-benzenedithiolate and L• = 1,2-benzenedithiolate radical monoanion) in the near-infrared and display frequencies around 1035 cm^{-1} in the infrared (KBr) indicating the presence of one (L•) radical, as elucidated by Wieghardt and co-workers.[20] Presumably, the less electron-donating sulfinate ligand coordinated to the {Fe(NO)} core of complexes **4**−**6** triggers the intramolecular electron transfer from the "redox-noninnocent" dithiophenolato(2−) to the {Fe(NO)} core to stabilize complexes **4**−**6**.[20] On the basis of UV−vis spectral, electron spin resonance, X-ray structural, and magnetic data, the electronic structures of the {Fe(NO)} cores of complexes **4**−**6** are best described as a $\{Fe^I(NO^+)\}^7$ (a d^7 $Fe^I(NO^+)$) core coordinated by one $[S,SO_2\text{-}C_6H_3R]^{2-}$ ligand as well as one dithio-*o*-semibenzoquinone(−) radical).[20]

X-ray crystal structures of complexes **5** and **6** are depicted in Figures 1 and 2, respectively, and selected bond dimensions for both complexes are presented in the figure captions.

(15) Grapperhaus, C. A.; Darensbourg, M. Y. *Acc. Chem. Res*. **1998**, *31*, 451.
(16) Kumar, M.; Colpas, G. J.; Day, R. O.; Maroney, M. J. *J. Am. Chem. Soc*. **1989**, *111*, 8323.
(17) Farmer, P. J.; Verpeaux, J.-N.; Amatore, C.; Darensbourg, M. Y.; Musie, G. *J. Am. Chem. Soc*. **1994**, *116*, 9355.
(18) McCleverty, J. A. *Chem. Rev*. **2004**, *104*, 403.
(19) Eisenberg, R.; Meyer, C. D. *Acc. Chem. Res*. **1975**, *8*, 26.
(20) (a) Ray, K.; Bill, E.; Weyhermuller, T. Wieghardt, K. *J. Am. Chem. Soc*. **2005**, *127*, 5641. (b) Herebian, D.; Bothe, E.; Bill, E.; Weyhermuller, T.; Wieghardt, K. *J. Am. Chem. Soc*. **2001**, *123*, 10012. (c) Sun, X.; Chun, H.; Hildenbrand, K.; Bothe, E.; Weyhermuller, T.; Neese, F.; Wieghardt, K. *Inorg. Chem*. **2002**, *41*, 4295. (d) Hsieh, C.-H.; Hsu, I.-J.; Lee, C.-M.; Ke, S.-C.; Wang, T.-Y.; Lee, G.-H.; Wang, Y.; Chen, J.-M.; Lee, J.-F.; Liaw, W.-F. *Inorg. Chem*. **2003**, *42*, 3925.

Table 1. Selected Infrared Data for Complexes **1**−**12** and Fe-NHase[12]

compds	ν_{NO} (cm^{-1}, KBr)	ν_{SO} (cm^{-1}, KBr)
1	1776	
2	1763	
3	1796	
4	1779	1196, 1060
5	1761	1202, 1057
6	1844 (m), 1801 (s)	1217, 1083
7	1636	1160, 1020
8	1648	1146, 1022
9	1661	1156, 1035
10	1605	
11	1606	
12	1615	
Fe-NHase	1853[a]	

[a] Measured in phosphate buffer (pH = 7.5).[12]

Geometry of the iron center in complex **4** is best described as a distorted trigonal bipyramidal coordination environment with NO and sulfinate groups occupying equatorial and axial positions, respectively.[13] In comparison, the geometry of iron center in complex **5** is a distorted geometry midway between tetragonal pyramid and trigonal bipyramid, whereas the distorted octahedral structure is adopted in complex **6**. Presumably, the lengthening in average Fe−N(O) bond lengths (1.599(2) vs 1.629(3) Å (**1** vs **4**), 1.606(3) vs 1.622(5) Å (**2** vs **5**), and 1.596(3) vs 1.651(2) Å (**3** vs **6**)) are caused by electronic perturbations from sulfur oxygenation and the induced intramolecular electron transfer from the coordinated dithiophenolato(2−) ligand to the {Fe(NO)} core. Consistent with other published transition-metal sulfinate complexes,[15] the S−O bond lengths average ca. 1.405(6) and 1.455(2) Å in complexes **5** and **6**, respectively.

Reduction of Complexes 4−6. When CH_3CN−THF solutions of complexes **4**−**6**, respectively, were treated with 1 equiv of $[RS]^-$ (R = Et, *o*-C_6H_4-NH_2), a pronounced change in color of the solution from dark purple to dark green accompanied by the dark yellow green precipitate was observed at ambient temperature. Instead of the direct nucleophilic attack of $[SEt]^-$ on the coordinated NO^+ yielding EtSNO and $[Fe(S,SO_2\text{-}C_6H_3R)(S,S\text{-}C_6H_3R)]_2^{2-}$, UV−vis, IR spectra, and X-ray diffraction studies confirmed the formation of the dianionic, mononuclear $\{Fe(NO)\}^7$ $[(NO)Fe(S,SO_2\text{-}C_6H_3R)(S,S\text{-}C_6H_3R)]^{2-}$ (R = H (**7**), *m*-CH_3 (**8**)) and $[(NO)Fe(S,SO_2\text{-}C_6H_2\text{-}3,6\text{-}Cl_2)(S,S\text{-}C_6H_2\text{-}3,6\text{-}Cl_2)]^{2-}$ (**9**) accompanied by a byproduct of $(SEt)_2$ identified by ^{1}H NMR (Scheme 1b). The infrared spectra show bands at 1636 and 1160, 1020 cm^{-1} (KBr) (**7**) (1648 and 1146, 1022 cm^{-1} (KBr) (**8**); 1661 and 1156, 1035 cm^{-1} (KBr) (**9**)) (Table 1) corresponding to the ν(NO) and ν(SO) stretching frequencies of the S-bonded sulfinate group, respectively.[15] The lower energy ν(NO) bands of complexes **7**−**9** shifted by ∼140 cm^{-1} from those of complexes **4**−**6** also imply the reduction process occurred in the {Fe(NO)} core. The proton chemical shifts of 1,2-benzenedithiolate ligands of complexes **7**−**9** were not observed in NMR spectra at room temperature. The effective magnetic moment was 1.76 and 1.85 μ_B for complexes **7** and **9**, respectively. No optical evidence (based on the UV−vis spectrum) for the presence of $[S,S\text{-}C_6H_3R]^{\bullet-}$ was observed. It is believed that relief of the electron deficiency due to reduction does not require electronic compensation from the "redox-noninnocent" dithiophenolate-(2−) ligand to the $\{Fe(NO)\}^7$ core any more. These results indicate that electronic structure of the $\{Fe(NO)\}^7$ core may exist as a low-spin d^6 Fe(II) (S = 0) coordinated by NO• radical (S = 1/2) to produce the total spin state of 1/2, i.e., the $\{Fe(NO)\}^7$ **7**−**9** having a low-spin d^6 Fe(II)−NO• radical electronic configuration in a distorted square pyramidal ligand field[18] even although that the intermediate-spin Fe^{III} (S = 3/2) antiferromagnetically coupled to coordinated triplet NO^- (S = 1) cannot be unambiguously ruled out.[14,18,19]

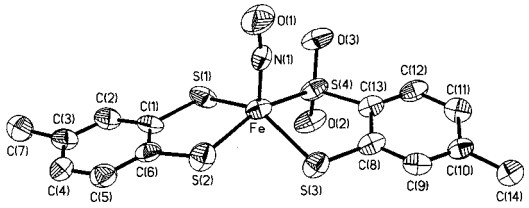

Figure 3. ORTEP drawing and labeling scheme of complex **8**. Selected bonds (Å): Fe−N(1), 1.659(6); Fe−S(1), 2.241(2); Fe−S(2), 2.259(2); Fe−S(3), 2.278(2); Fe−S(4), 2.249(2); N(1)−O(1), 1.158(7) Å. Selected angles (deg): Fe−N(1)−O(1), 171.6(6); S(1)−Fe−S(3), 144.04(9); S(4)−Fe−S(2), 158.35(9); S(1)−Fe−S(2), 88.24(8); S(3)−Fe−S(4), 86.66(7); N(1)−Fe−S(1), 108.1(2); N(1)−Fe−S(2), 102.9(2); N(1)−Fe−S(3), 107.9(2); N(1)−Fe−S(4), 98.7(2).

Figure 3 displays the thermal ellipsoid plot of the dianionic complex **8**, and selected bond distances and angles are given in the figure captions. Analysis of the bond angles for complexes **7**−**9** reveals that coordination geometry of the iron center is best described as a distorted square pyramid with a bent apical NO, and the iron atom is displaced from the mean four sulfur atom plane (0.5382 vs 0.5462 Å for **4** vs **7**, 0.5492 vs 0.5590 Å for **5** vs **8**, and 0.4947 vs 0.5168 Å for **6** vs **9**). In contrast to the linear Fe−N−O bonds of complexes **4**−**6**, the slightly bent Fe−N−O bonds with angles of 156.8(9), 168.0(7), and 166.0(8)° for complexes **7**−**9**, respectively, also support the presence of $\{Fe^{II}(\bullet NO)\}^7$ electronic configuration.[18] Geometry around the Fe center responding rapidly to the electronic change of the {Fe(NO)} core may be rationalized according to the studies on the qualitative MO energy level orderings for the five-coordinated $\{Fe(NO)\}^{6/7}$ metal−nitrosyl complexes.[19] Computational studies have suggested that geometrical change from square pyramidal with linear apical NO to square pyramidal with bent apical NO or trigonal bipyramidal with linear equatorial NO may occur for a five-coordinated metal−nitrosyl complex upon the electronic changes going from $\{Fe(NO)\}^6$ to $\{Fe(NO)\}^7$.[19] Compared to complexes **4**−**6**, the electronic effect (from $\{Fe(NO)\}^6$ to $\{Fe(NO)\}^7$) may explain the observed lengthening of the average Fe−N(O) bond lengths (average 1.634 (**4**−**6**) vs average 1.672 Å (**7**−**9**)) in complexes **7**−**9**.[18] As shown in Table 2, the N−O bond lengths of 1.149(10) and 1.158(7) Å in complexes **8** and **9**, respectively, are comparable to the N−O bond distance of 1.154 Å in free •NO but far from that of 1.26 Å in NO^-.[21]

(21) (a) Teillet-Billy, D.; Fiquet-Fayard, F. *J. Phys. Chem.* **1990**, *94*, 3450. (b) Wong, M. W.; Nobes, R. H.; Bouma, W. J.; Radom, L. *Chem. Phys.* **1989**, *91*, 2971.

Table 2. Selected Bond Distances (Å) and Angles (deg) for Complexes **1**−**12**

compds	Fe−N	N−O	S−O	−Fe−N−O
1	1.599(2)	1.66(3)		176.2(3)
2	1.606(3)	1.182(4)		176.0(3)
3	1.596(3)	1.163(4)		177.6(3)
4	1.629(3)	1.169(4)	1.469(2), 1.459(2)	171.0(3)
5	1.622(5)	1.162(6)	1.425(5), 1.385(6)	171.9(5)
6	1.651(2)	1.154(3)	1.443(2), 1.466(2)	177.1(2)
7[a]	1.779(9)	1.002(9)	1.429(8), 1.394(8)	156.8(8)
8	1.659(6)	1.158(7)	1.460(5), 1.501(5)	168.0(17)
9	1.684(8)	1.149(10)	1.462(9), 1.48(1)	166.0(8)
10[a]	1.712(6)	1.08(1)		160.5(6)
11	1.692(3)	1.193(4)		151.8(3)
12	1.702(5)	1.186(6)		153.4(4)

[a] The atoms Fe(1), N(1), O(1), O(2), and O(3) in **7** and Fe(1), N(1), and O(1) in **10** are structurally disordered at two equal occupancy locations.

Reduction of Complexes 1−3. To follow up on our earlier communication with a more complete understanding of the reactivity of the $\{Fe(NO)\}^n$ ($n = 6, 7$) nitrosylated iron−thiolates toward oxygen and their relevance as a model of oxygen binding to sulfur in the Fe-containing nitrile hydratase active site,[13] the $[(NO)Fe(S,S\text{-}C_6H_3R)_2]^{2-}$ (R = H (**10**), *m*-CH_3 (**11**)) and $[(NO)Fe(S,S\text{-}C_6H_2\text{-}3,6\text{-}Cl_2)_2]^{2-}$ (**12**) complexes with the $\{Fe(NO)\}^7$ electronic core were synthesized by addition of $[SEt]^-$ to complexes **1**−**3**, respectively, in THF at ambient temperature (Scheme 1c). The most noteworthy characteristic of reduction of complexes **1**−**3** is the disappearance of a low-energy absorption band at 1304 nm (**1**) (1300 nm (**2**), 1248 nm (**3**)) with concomitant formation of a 684 nm absorption band (**10**) (684 nm (**11**), 670 nm (**12**)). The ν(NO) stretching frequencies of complexes **10**−**12** (1605 (**10**), 1606 (**11**), and 1615 (**12**) cm^{-1} (KBr)) fall into the range (1620−1675 cm^{-1}) observed for five-coordinated iron−nitrosyl complexes having the $\{Fe(NO)\}^7$ configuration with $S = 1/2$ ground state.[18] The proton chemical shift of 1,2-benzenedithiolate ligands of complexes **10**−**12** was not observed in the NMR spectra at ambient temperature. The effective magnetic moment is 2.2 and 2.1 μ_B for complexes **10** and **12**, respectively. Electrochemistry of complex **12** (2.5 mM), measured in CH_3CN with 0.1 M [*n*-Bu_4N][PF_6] as supporting electrolyte (scan rate 100 mV/s), reveals one reversible oxidation−reduction process at −0.554 V ($E_{1/2}$ vs $Ag/AgNO_3$), as compared to −0.365 V for complex **9** (2.5 mM) (Figure 4).

The X-ray crystal structure of complex **12** is displayed in Figure 5, and selected bond distances and angles are presented in the figure captions. The Fe−N−O bond angles of 160.5(6), 151.8(3), and 153.4(4)° for complexes **10**−**12** are similar to those of their five-coordinated analogues, averaging 160° in $\{Fe(NO)\}^7$ species containing the $[S_4]$ donor atom set.[18] The changes in Fe−N−O bond angle from the bent form (151.8(3) and 153.4(4)° for complexes **11** and **12**, respectively) to the less bent form (168.0(7) and 166.0(8)° for complexes **8** and **9**, respectively) are, presumably, caused by electronic perturbation from sulfur oxygenation (Table 2). In contrast to the lengthening of the average Fe−N(O) bond length caused by sulfur oxygenation accompanied by the induced electron-transfer from dithiophenolate(2−) to the {Fe(NO)} core in complexes **4**−**6**, the relief of the electron

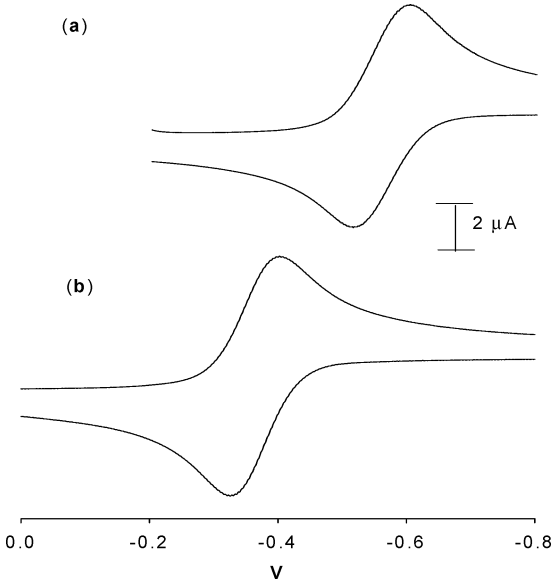

Figure 4. Cyclic voltammograms (at 100 mV/s) of (a) complex **12** (one reversible redox process at −0.554 V ($E_{1/2}$ vs $Ag/AgNO_3$)) and (b) complex **9** (one reversible redox process at −0.365 V ($E_{1/2}$ vs $Ag/AgNO_3$)) in CH_3CN solution with 0.1 M [*n*-Bu_4N][PF_6] as supporting electrolyte at 25 °C.

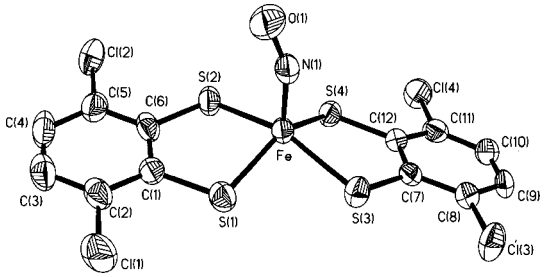

Figure 5. ORTEP drawing and labeling scheme of complex **12**. Selected bonds (Å): Fe−N(1), 1.702(5); Fe−S(av), 2.2527(16); N(1)−O(1), 1.186(6). Selected angles (deg): Fe−N(1)−O(1), 153.4(4); S(1)−Fe−S(4), 144.42(6); S(2)−Fe−S(3), 158.08(6); S(2)−Fe−S(1), 88.09(6); S(3)−Fe−S(4), 87.58(5); N(1)−Fe−S(1), 106.48(16); N(1)−Fe−S(2), 96.47(16); N(1)−Fe−S(3), 105.45(16); N(1)−Fe−S(4), 108.99(16).

deficiency from reduction in combination with the less electron-donating sulfinate in $\{Fe(NO)\}^7$ complexes **8** and **9** may explain the observed shortening of the average Fe−N(O) bond lengths from complexes **11** and **12** to complexes **8** and **9** (the average Fe−N(O) bond length of 1.697(5) Å in complexes **11** and **12** vs the average Fe−N(O) bond length of 1.672(8) Å in complexes **8** and **9**). It is also noticed that the N−O bond lengths of 1.193(4) and 1.186(6) Å in complexes **11** and **12**, longer than those of 1.158(7) and 1.149(10) Å in complexes **8** and **9**, are nearly midway between the N−O bond distance of 1.154 Å in free •NO and 1.26 Å in NO^- (Table 2).[21] Therefore, the electronic structures of the $\{Fe(NO)\}^7$ core of complexes **10**−**12** are best described in terms of having $\{Fe^{II}(\bullet NO)\}^7$ (a low-spin d^6 Fe^{II} ($S = 0$) coordinated by NO• ($S = 1/2$) radical in a distorted square pyramidal ligand field) or the having presence of a resonance hybrid of $\{Fe^{II}(\bullet NO)\}^7$ and $\{Fe^{III}(NO^-)\}$.[7,18,19]

Photochemical Studies of the $\{Fe(NO)\}^{6/7}$ Complexes. NO release upon photolysis has been observed in the {Fe-

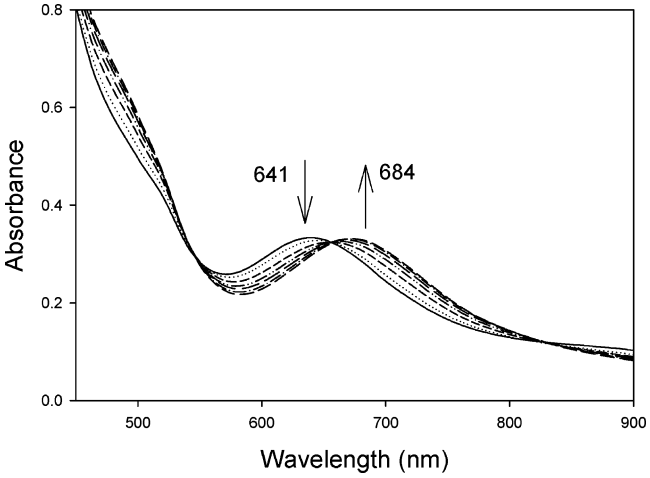

Figure 6. Conversion of complex **7** (0.1 mM in CH_3CN solution) to **10** monitored by UV−vis spectrometry under irradiation (Hg lamp, I_{max} = 366 nm). The absorption band at 684 nm (**10**) increases with decrease of the band at 641 nm (**7**), and an isosbestic point was observed.

(NO)}^{6} complexes.[22] The absorption band (497 nm for **1**, 500 nm for **2** and **3**) decays after irradiation (Hg lamp, I_{max} = 366 nm) of CH_2Cl_2 (THF) solution of complexes **1**−**3** (0.1 mM) for 30 min and yields an insoluble, uncharacterized yellow solid. In contrast to photolability of NO (decomposition) in complexes **1**−**3**, irradiation of CH_3CN solution of complexes **10**−**12** did not cause dissociation of the bound NO. Photolysis (Hg lamp, I_{max} = 417 nm) of a CH_2Cl_2 solution of complex **4** yielded complex **1** with $k_{obs} = 4.8 \times 10^{-4}$ s^{-1} (25 ± 2 °C), compared to photolysis of CH_2Cl_2 solution of complex **4** in the presence of triphenylphosphine (1200-fold) with $k_{obs} = 6.3 \times 10^{-4}$ s^{-1} (25 ± 2 °C). Obviously, the presence of triphenylphosphine in the photochemical removal of oxygen of complex **4** did not greatly accelerate the rate of the deoxygenation reaction. The dianionic S-bonded monosulfinate complexes **7**−**9** also undergo oxygen transfer reaction in CH_3CN solution with 2 equiv of PPh_3 over the course of 4 days to yield complexes **10**−**12**, respectively, and triphenylphosphine oxide identified by ^{31}P NMR spectroscopy. In addition, the transformation of complexes **7**−**9** to complexes **10**−**12** was also displayed when CH_3CN solutions of complexes **7**−**9** were photolyzed under N_2 purge at ambient temperature (Scheme 1d). The quantitative conversion of complex **7** to **10** was also monitored by UV−vis spectrometry under irradiation (Hg lamp, I_{max}= 366 nm); the band at 641 nm (complex **7**) (630 nm, complex **9**) disappeared accompanied by the simultaneous formation of one intense absorption band at 684 nm (complex **10**) (670 nm, complex **12**) and the color changed from dark green to brown yellow. The isosbestic point was observed in successive optical spectra, as shown in Figure 6. During this transformation, no product with NO dissociation was detected spectrally. In contrast to complexes **4**−**6** possessing photolabile [O] atoms of the sulfinate ligand and the photolabile NO, the direct transformation of complexes **7**−**9** to **10**−**12**, respectively, under irradiation was ascribed

Scheme 2

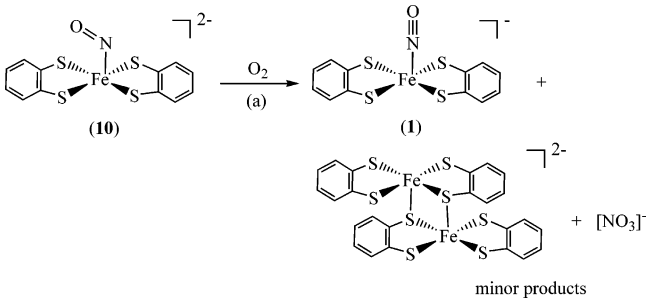

to the photochemically inert {Fe(NO)}^{7} electronic core.[22] These results demonstrated that the [O] atoms of the coordinated-sulfinate ligand are photolabile in both {Fe(NO)}^{6} and {Fe(NO)}^{7} iron−nitrosyl−sulfinate complexes under irradiation.[13]

Oxidation of the {Fe(NO)}^{7} Complexes. When a CH_3CN solution of complexes **10**/**12** was stirred with 1 equiv of dioxygen under controlled conditions at room temperature, a pronounced color change from dark green to dark red brown occurred. The UV−vis, IR, and X-ray diffraction studies confirmed the formation of complexes **1**/**3** (major product) accompanied by byproducts $[NO_3]^-$ and the dimeric $[Fe(S,S\text{-}C_6H_3R)_2]_2^{2-}$ (minor product) (Scheme 2). Reactions carried out by using $^{18}O_2$ demonstrate that O_2 is the source of the $[NO_3]^-$. The infrared spectrum displays ν_{NO} vibrational bands at 1363 and 1374 cm^{-1} (KBr), shifting from 1384 cm^{-1} (KBr), in the isotopic labeling experiments. It has been shown that nitrosyl heme iron enzymes (nitrosylhemoglobin and nitrosylmyoglobin) oxidized to metHb and deoxyMb by O_2 generate nitrate in vivo.[23a,b] The influence of the electronic structure of the {Fe(NO)}$^{6/7}$ core on the chemical features of complexes **1**−**3** vs **10**−**12** is clearly reflected in the oxygen reaction: complexes **1**−**3** with {Fe(NO)}^{6} core promote electrophilic attack of O_2 on sulfur and O_2 activation to yield the S-bonded monosulfinate iron−nitrosyl species (complexes **4**−**6**), whereas an attack of O_2 on the {Fe(NO)}^{7} complexes **10**−**12** lead to the formation of complexes **1**−**3** (yield 84% for **10**, 72% for **12**) and the minor products $[Fe(S,S\text{-}C_6H_3R)_2]_2^{2-}$ and $[NO_3]^-$ (yield 9% for **10**, 11% for **12**). Thus, the electronic structure of the {Fe(NO)}^{n} center appears crucial for promoting oxygenation at either the sulfur or the NO site.

In contrast to the electrophilic attack of O_2 on •NO of complexes **10**/**12**, the direct conversion of complexes **7**−**9** to complexes **4**−**6** was observed when CH_3CN solutions of complexes **7**−**9** were treated with O_2 at ambient temperature. Obviously, these iron−sulfinate nitrosyl complexes containing the {Fe(NO)}^{7} core undergo a reversible one-electron redox process (Scheme 1b′). Consistent with complex $[(C_4H_8O)Fe(S,S\text{-}C_6H_4)_2]^-$, complex $[Fe(S,S\text{-}C_6H_4)_2]^{2-}$ does not initiate O_2 activation to yield iron−sulfinate/−sulfenate

(22) (a) Patra, A. K.; Afshar, R.; Olmstead, M. M.; Mascharak, P. K. *Angew. Chem., Int. Ed.* **2002**, *41*, 2512. (b) Afshar, R. K.; Patra, A. K.; Olmstead, M. O.; Mascharak, P. K. *Inorg. Chem.* **2004**, *43*, 5736.

(23) (a) Herold, S.; Röck, G. *Biochemistry* **2005**, *44*, ASAP. (b) Bruun-Jensen, L.; Skibsted, L. H. *Meat Sci.* **1996**, *44*, 145. (c) Clarkson, S. G.; Basolo, F. *Inorg. Chem.* **1973**, *12*, 1528. (d) Ford, P. C.; Lorkovic, I. M. *Chem. Rev.* **2002**, *102*, 993. (e) Trogler, W. C.; Marzilli, L. G. *Inorg. Chem.* **1974**, *13*, 1008. (f) Kubota, M.; Phillips, D. A. *J. Am. Chem. Soc.* **1975**, *97*, 5637.

compounds identified by IR ν(SO); instead, a dimeric $[Fe(S,S\text{-}C_6H_4)_2]_2^{2-}$ formed after the reaction solution of $[Fe(S,S\text{-}C_6H_4)_2]^{2-}$ and O_2 was stirred in CH_2Cl_2 for 1 min.

Conclusion and Comments

Studies on the mononuclear iron−sulfinate nitrosyl and iron−thiolate nitrosyl complexes (**1**−**12**) with the $\{Fe(NO)\}^{6/7}$ core have led to the following results:

(1) Monoanionic complexes **1**−**3** with the $\{Fe(NO)\}^6$ core initiate sulfur oxygenation of iron−thiolate by molecular oxygen to yield S-bonded monosulfinate iron complexes **4**−**6** via the proposed intermediate **A** (below), whereas dianionic complexes **10**−**12** with the $\{Fe(NO)\}^7$ core triggers, to a certain extent, the attack of O_2 on the •NO radical of the $[Fe^{II}\text{-}NO\bullet]$ core yielding complexes **1**−**3** accompanied by the minor products $[NO_3]^-$ and $[Fe(S,S\text{-}C_6H_3R)_2]_2^{2-}$ via the proposed intermediate **B** (below).[23c−f] In the studies of reaction of dioxygen and nitrosyl Co^{II}−Schiff base complexes, coordination of dioxygen to the N atom of the NO group is the rate-determining step, leading to an intermediate $\{Co^{II}N(O)(\eta_1\text{-}O_2)\}$.[23c] The proposed species, $CoN(O)(\eta_1\text{-}O_2)$, gains supports from the fact that the reaction rate increases with increase electron density at the nitrosyl site. One electron reduction of the $\{Fe(NO)\}^6$ complexes **1**−**3** increases electron density about the $\{Fe(NO)\}$ core of the complexes **10**−**12**. Higher electron density facilitates oxidation of the nitrosyl group in the $\{Fe(NO)\}^7$ complexes **10**−**12**. It also explains why sulfur oxygenation occurs in the $\{Fe(NO)\}^6$ complexes **1**−**3** instead of the nitrate formation. To our knowledge, two transition metal nitrato complexes, nitrato cobaloxime[23e] and $Ir(PPh_3)_2(CO)ClX(NO_3)$,[23f] have been reported.

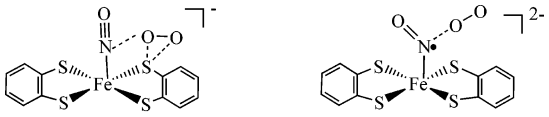

(A) (B)

(2) The less electron-donating sulfinate coordinated to the $\{Fe(NO)\}^7$ core stabilizing the dianionic S-bonded monosulfinate iron species **7**−**9** was employed to explain that the NO group of complexes **10**−**12** are much more O_2-sensitive than the corresponding complexes **7**−**9**. The electronic perturbation of the $\{Fe(NO)\}^7$ core caused by the coordinated sulfinate ligand in complexes **7**−**9** serves to regulate the reactivity of complexes **7**−**9** toward O_2. In contrast to the attack of O_2 on the •NO radical of the $\{Fe(NO)\}^7$ core of complex **10** yielding complex **1** along with the minor products $[NO_3]^-$ and $[Fe(S,S\text{-}C_6H_4)_2]_2^{2-}$, complexes **7**−**9** with less electron-donating sulfinate ligand coordinated to iron were oxidized by O_2 to yield complexes **4**−**6**, respectively. Presumably, factors contributing to the distinct oxidation pathways are attributed to the less electron-donating sulfinate ligand sufficient to place the $\{Fe(NO)\}^7$ core in a $\{Fe^{II}(\bullet NO)\}^7$ condition but insufficient to cause the formation of a resonance hybrid of the $\{Fe^{II}(\bullet NO)\}^7$ and $\{Fe^{III}(NO^-)\}^7$ states, as implicated in the N−O bond distances of complexes **11** and **12** vs **8** and **9**.

(3) In the $\{Fe(NO)\}^6$ system, the lengthenings in average Fe−N(O) bond lengths are caused by sulfur oxygenation accompanied by the induced electron rearrangement from dithiophenolato(2−) ligand to the $\{Fe(NO)\}$ core (Table 2). However, the Fe−N−O bond angle is not affected by the sulfur oxygenation. In the $\{Fe(NO)\}^7$ system, the shorter Fe−N(O) bond distances are observed as a consequence of substitution of thiolate ligand by the corresponding S-bonded sulfinate ligand, as observed in the iron−thiolate $\{Fe(NO)\}^7$ complexes **11** and **12** (Fe−N = 1.692(3) Å (**11**), Fe−N = 1.702(5) Å (**12**)) and iron−sulfinate $\{Fe(NO)\}^7$ complexes **8** and **9** (Fe−N = 1.659(6) Å (**8**), Fe−N = 1.684(8) Å (**9**)) (Table 2). The influence of sulfinate ligand on the electronic environment of the $\{Fe(NO)\}^7$ core is also reflected in the change of Fe−N−O bond angle of complexes **11** and **12** vs **8** and **9** from a bent form (average 152.6(4)° for complexes **11** and **12**) to a less bent form (average 167.0(17)° for complexes **8** and **9**).

(4) The presence of NO binding to the iron center forming $\{Fe(NO)\}^6$ iron−thiolate nitrosyl complexes appears crucial in initiating oxygenation at sulfur and resulting in the thermally stable S-bonded monosulfinate iron species.

(5) The iron−sulfinate nitrosyl species with the $\{Fe(NO)\}^{6/7}$ electronic core exhibit the photolabilization of sulfur-bound [O] moiety under irradiation, and the sulfinate ligand coordinated to the $\{Fe(NO)\}^{6/7}$ core does not promote the photolability of the Fe−NO bond.

(6) X-ray structural data, magnetic measurements showing diamagnetic properties and EPR silence, and IR and UV−vis spectra suggest that the electronic structures of complexes **4**−**6** are best described as a $[(NO^+)Fe^I$(dithio-*o*-semibenzoquinone(−) radical)(sulfinato−thiophenolato(2−))$]^-$ (**C**).[18,20]

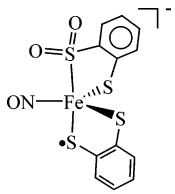

(C)

It has been known that the inactive NO-bound form of Fe-NHase with the iron center coordinated by two modified cysteines residues (sulfinate RSO_2^- and sulfenate RSO^- groups) through sulfur atoms and one NO is generated in cells grown in the dark and the active form is regenerated with release of NO and [O] molecules upon exposure to light.[6−8] As shown in Scheme 3, the biomimetic reaction cycle of complexes **1**−**4**−**7**−**10** (or complexes **2**−**5**−**8**−**11** and **3**−**6**−**9**−**12**) may provide some clues to the transformation mechanism between the active form and inactive NO-bound form of Fe-NHase.

On the basis of this study, we speculate that the interconversion between the active and inactive NO-bound forms of Fe-NHase may involve intramolecular $\{FeNO\}^6 \leftrightarrow \{FeNO\}^7$ electron-rearrangement processes.[5−8]

Scheme 3

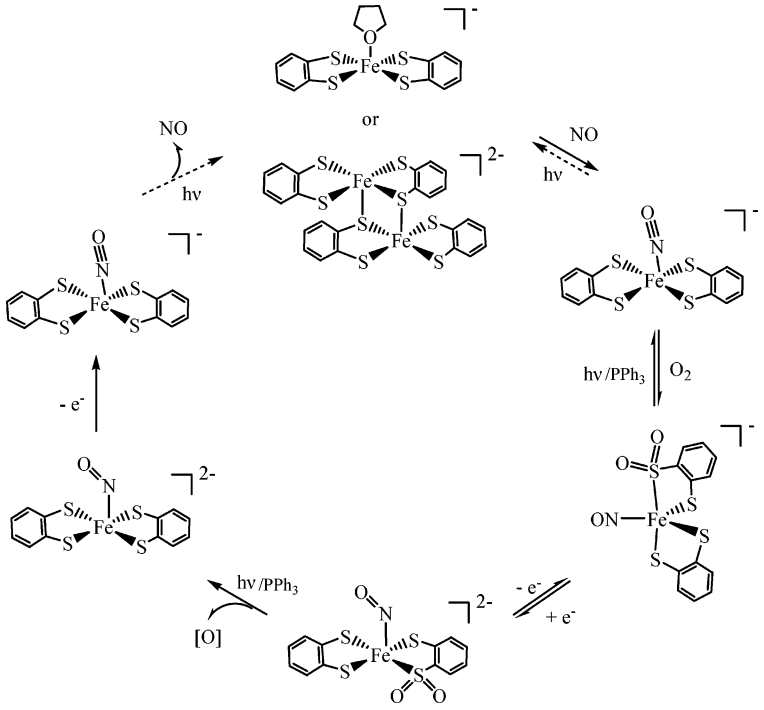

Experimental Section

Manipulations, reactions, and transfers were conducted under nitrogen according to Schlenk techniques or in a glovebox (argon gas). Solvents were distilled under nitrogen from appropriate drying agents (diethyl ether from CaH_2; acetonitrile from $CaH_2-P_2O_5$; methylene chloride from P_2O_5; hexane and tetrahydrofuran (THF) from sodium benzophenone) and stored in dried, N_2-filled flasks over 4 Å molecular sieves. Nitrogen was purged through these solvents before use. Solvent was transferred to the reaction vessel via stainless cannula under positive pressure of N_2. The reagents iron pentacarbonyl, 1,2-benzenedithiol, toluene-3,4-dithiol, 3,6-dichloro-1,2-benzenedithiol, 2-aminobenzenethiol, and bis(triphenylphosphoranylidene)ammonium chloride ([PPN][Cl]) were used as received. [PPN][NO_2] and [PPN][$Fe(CO)_3(NO)$] were prepared by published procedures.[24] Infrared spectra of ν(NO) and ν(SO) stretching frequencies were recorded on a Perkin-Elmer model spectrum one B spectrophotometer with sealed solution cells (0.1 mm) and KBr windows. UV−vis spectra were recorded on GBC Cintra 10e and Jasco V-570 spectrometers. ^{1}H NMR spectra were obtained on a Varian Unity-400 spectrometer. Cyclic voltammograms were obtained from 2.5 mM analyte concentration in CH_3CN using 0.1 M [*n*-Bu_4N][PF_6] as a supporting electrolyte. Potentials were measured at 298 K vs a $Ag/AgNO_3$ reference electrode by using a Pt working electrode. Under the conditions employed, the potential (V) of the ferrocenium/ferrocene couple was 0.16 (CH_3CN). Analyses of carbon, hydrogen, and nitrogen were obtained with a CHN analyzer (Heraeus).

Preparation of [PPN][(NO)Fe(S,S-C_6H_2-3,6-Cl_2)$_2$] (3). A 10 mL volume of air was injected into the THF solution (10 mL) containing [PPN][$Fe(CO)_3(NO)$] (0.4 mmol, 0.283 g) and 3,6-dichloro-1,2-benzenedithiol (0.8 mmol, 0.169 g) at ambient temperature. After the mixture solution was stirred for 3 days, the reaction solution was filtered through Celite and 20 mL hexane was added to precipitate the dark red solid [PPN][(NO)Fe(S,S-C_6H_2-3,6-Cl_2)$_2$] (**3**) (0.363 g, 87%).[13] Diffusion of hexane into a THF solution of complexes **3** at −15 °C for 4 weeks led to red crystals suitable for X-ray crystallography. IR(THF): 1802 vs (ν_{NO}) cm^{-1}. ^{1}H NMR (CD_2Cl_2): δ 7.612−7.637 (m), 7.418−4.746 (m), 7.075 (s) ppm. Absorption spectrum (CH_2Cl_2) [λ_{max}, nm (ϵ, M^{-1} cm^{-1})]: 324 (26 841), 500 (3957), 1248 (5603). Anal. Calcd for $C_{48}H_{34}OS_4N_2P_2Cl_4Fe$: C, 55.29; H, 3.29; N, 2.69. Found: C, 55.44; H, 3.54; N, 2.80.

Preparation of [PPN][(NO)Fe(S,SO_2-C_6H_3-*m*-CH_3)(S,S-C_6H_3-*m*-CH_3)] (5) and [PPN]$_2$[(NO)Fe(S,SO_2-C_6H_2-3,6-Cl_2)(S,S-C_6H_2-3,6-Cl_2)]$_2$ (6).[13] To a THF solution (10 mL) of complex 2 (0.373 g, 0.4 mmol) (complex 3 (0.416 g, 0.4 mmol)) was bubbled dry O_2 was bubbled until the mixture solution became purple (1 week) at room temperature. Hexane (20 mL) was added to precipitate the purple solid, and then the purple solid was redissolved in CH_2Cl_2. Purification using silica gel chromatography with CH_2Cl_2 as the eluent first gave a trace of yellow-green band, and a reddish brown band collected that was identified as the unreacted complex 2 (**3**). The eluent was then changed to THF and the purple product eluted from the column. The purple solution was reduced in volume under vacuum, and hexane was added to precipitate the purple solid [PPN][(NO)Fe(S,SO_2-C_6H_3-*m*-CH_3)(S,S-C_6H_3-*m*-CH_3)] (5) (0.078 g, 20%) ([PPN]$_2$[(NO)Fe(S,SO_2-C_6H_2-3,6-Cl_2)(S,S-C_6H_2-3,6-Cl_2)]$_2$ (6) (0.077 g, 18%)). Recrystallization by diffusion of diethyl ether into a concentrated THF solution of complex 5 (CH_3CN solution of complex 6) at −15 °C for 4 weeks afforded the purple crystals suitable for X-ray diffraction analysis. Complex **5**: IR 1786 (ν_{NO}) cm^{-1} (THF), 1761 (ν_{NO}), 1202, 1057 (ν_{SO}) (KBr) cm^{-1}; ^{1}H NMR (CD_2Cl_2) δ 7.95 (d), 7.89 (s), 7.50 (d), 7.11 (d), 7.00 (d), 6.86 (d), 2.38 (s), 2.29 (d) (S,S-C_6H_3-*m*-CH_3, S,S(O)$_2$-C_6H_4-*m*-CH_3) ppm; absorption spectrum (THF) [λ_{max}, nm (ϵ, M^{-1} cm^{-1})] 315 (25 868), 535 (3809), 995 (3615). Complex **6**: IR 1803 (ν_{NO}) cm^{-1} (THF), 1844, 1801 (ν_{NO}), 1217, 1083 (ν_{SO}) (KBr) cm^{-1}; ^{1}H NMR ($CDCl_3$) δ 7.227 (d), 7.015 (d), 6.995 (d) (S,S-C_6H_2-Cl_2, S,S(O)$_2$-C_6H_4-Cl_2) ppm; absorption spectrum (CH_2Cl_2) [λ_{max}, nm (ϵ, M^{-1} cm^{-1})] 316

(24) (a) Hedberg, L.; Hedberg, K.; Satija, S. K.; Swanson, B. I. *Inorg. Chem.* **1985**, *24*, 2766. (b) Albano, V. G.; Araneo, A.; Bellon, P. L.; Ciani, G.; Manassero, M. *J. Organomet. Chem.* **1974**, *67*, 413.

(43 991), 528 (8109), 974 (6756). Anal. Calcd for $C_{96}H_{68}O_6N_4P_4S_8Cl_8Fe_2$: C, 53.65; H, 3.19; N, 2.61. Found: C, 53.83; H, 3.61; N, 2.62.

Preparation of [PPN]$_2$[(NO)Fe(S,SO$_2$-C$_6$H$_3$R)(S,S-C$_6$H$_3$R)] (R = H (7), *m*-CH$_3$ (8)) and [PPN]$_2$[(NO)Fe(S,SO$_2$-C$_6$H$_2$-3,6-Cl$_2$)-(S,S-C$_6$H$_2$-3,6-Cl$_2$)] (9).[13] To a Schlenk tube containing [PPN][S,-NH$_2$-C$_6$H$_4$] (0.133 g, 0.2 mmol) was added the THF solution (7 mL) of complex **4** (0.188 g, 0.2 mmol) (complex **5**, 0.193 g, 0.2 mmol; complex **6**, 0.215 g, 0.1 mmol) under N_2 at ambient temperature. After the reaction solution was stirred overnight, the mixture solution was stood for 30 min to precipitate the dark green solid. The upper yellow solution was transferred to another flask and then dried under vacuum to obtain the (S,NH$_2$-C$_6$H$_4$)$_2$ solid identified by ^{1}H NMR. Then THF (15 mL) was added to wash the dark green solid twice. The green solid was dried under N_2 purge to afford the product [PPN]$_2$[(NO)Fe(S,SO$_2$-C$_6$H$_4$)(S,S-C$_6$H$_4$)] (**7**) (0.268 g, 91%) ([PPN]$_2$[(NO)Fe(S,SO$_2$-C$_6$H$_3$-*m*-CH$_3$)(S,S-C$_6$H$_3$-*m*-CH$_3$)] (**8**) (0.335 g, 90%); [PPN]$_2$[(NO)Fe(S,SO$_2$-C$_6$H$_2$-3,6-Cl$_2$)-(S,S-C$_6$H$_2$-3,6-Cl$_2$)] (**9**) (0.142 g, 44%)). Diffusion of diethyl ether into a CH$_3$CN solution of complexes **7** (**8**, **9**) at −15 °C for 4 weeks led to dark green crystals suitable for X-ray diffraction. Complex 7: IR 1636 (ν_{NO}), 1160, 1020 (ν_{SO}) cm^{-1} (KBr); absorption spectrum (CH$_3$CN) [λ_{max}, nm (ϵ, M^{-1} cm^{-1})] 412 (3200), 502 (1030), 641 (750), 877 (240). Anal. Calcd for $C_{84}H_{68}N_3O_3P_4S_4Fe$: C, 68.38; H, 4.65; N, 2.85. Found: C, 68.38; H, 4.92; N, 2.64. Complex **8**: IR 1648 (ν_{NO}), 1146, 1022 (ν_{SO}) (KBr) cm^{-1}; absorption spectrum (CH$_3$CN) [λ_{max}, nm (ϵ, M^{-1} cm^{-1})] 485 (2108), 660 (1158). Complex **9**: IR 1661 (ν_{NO}), 1156, 1035 (ν_{SO}) (KBr) cm^{-1}; absorption spectrum (CH$_2$Cl$_2$) [λ_{max}, nm (ϵ, M^{-1} cm^{-1})]: 332 (18 274), 426 (4122), 630 (1010), 932 (528). Anal. Calcd for $C_{84}H_{64}O_3S_4N_3P_4Cl_4Fe$: C, 62.54; H, 4.00; N, 2.60. Found: C, 61.24; H, 4.07; N, 3.16. The elemental analysis did not show good agreement with the calculated values because of the extreme air-sensitivity of sample **9**.

Preparation of [PPN]$_2$[(NO)Fe(S,S-C$_6$H$_3$R)$_2$] (R = H (10), *m*-CH$_3$ (11)) and [PPN]$_2$[(NO)Fe(S,S-C$_6$H$_2$-3,6-Cl$_2$)$_2$] (12). The degassed THF (10 mL) was added via cannula to the Schlenk tube containing [PPN][S,NH$_2$-C$_6$H$_4$] (0.133 g, 0.2 mmol) (or 0.018 g [Me$_4$N][BH$_4$] or 0.029 g [Et$_4$N][BH$_4$]) and complex **1** (0.181 g, 0.2 mmol) (complex **2** (0.186 g, 0.2 mmol); complex **3** (0.208 g, 0.2 mmol)) under N_2 at ambient temperature. The reaction solution was stirred for 2 h, and then stood for 30 min to precipitate the green-yellow solid. The upper yellow solution was transferred to another flask under positive N_2 pressure and then dried under vacuum to obtain the (S, NH$_2$-C$_6$H$_4$)$_2$ solid identified by ^{1}H NMR. The green-yellow solid was washed twice by THF and then dried under N_2 purge to afford the product [PPN]$_2$[(NO)Fe(S,S-C$_6$H$_4$)$_2$] (**10**) (0.246 g, 85%) ([PPN]$_2$[(NO)Fe(S,S-C$_6$H$_3$-*m*-CH$_3$)$_2$] (**11**) (0.335 g, 90%); [PPN]$_2$[(NO)Fe(S,S-C$_6$H$_2$-3,6-Cl$_2$)$_2$] (**12**) (0.251 g, 79%)). Diffusion of diethyl ether into a CH$_3$CN solution of complex **10** (**11**, **12**) at −15 °C for 4 weeks led to green crystals suitable for X-ray crystallography. Complex **10**: IR 1605 vs (ν_{NO}) cm^{-1} (KBr); absorption spectrum (CH$_3$CN) [λ_{max}, nm (ϵ, M^{-1} cm^{-1})] 405 (3380), 511 (930), 684 (710), 762 (460). Anal. Calcd for $C_{84}H_{68}N_3OP_4S_4Fe$: C, 69.89; H, 4.70; N, 2.91. Found: C, 69.80; H, 4.70; N, 2.94. Complex **11**: IR 1606 vs (ν_{NO}) cm^{-1} (KBr); absorption spectrum (CH$_3$CN) [λ_{max}, nm (ϵ, M^{-1} cm^{-1})] 420 (4829), 685 (1084). Complex **12**: IR 1615 vs (ν_{NO}) cm^{-1} (KBr); absorption spectrum (CH$_2$Cl$_2$) [λ_{max}, nm (ϵ, M^{-1} cm^{-1})] 340 (18 034), 420 (4688), 670 (764). Anal. Calcd for $C_{84}H_{64}OS_4N_3P_4Cl_4Fe$: C, 63.80; H, 4.08; N, 2.66. Found: C, 63.47; H, 4.07; N, 2.97.

Photolysis of CH$_2$Cl$_2$ Solutions of [PPN][(NO)Fe(S,S-C$_6$H$_4$)$_2$] (1). A 4 mL quartz reactor containing a CH$_2$Cl$_2$ solution (3 mL) of [PPN][(NO)Fe(S,S-C$_6$H$_4$)$_2$] (**1**) (0.1 mM) was sealed under positive N_2. The solution was then irradiated by a Hg lamp (8 W × 8, I_{max} = 366 nm) at room temperature. The reaction solution was monitored immediately by UV−vis. After 18 min of irradiation, the resulting light yellow solution accompanied by the insoluble yellow solid showed no absorption band in the UV−vis spectrum (also, no ν_{NO} peak in the IR spectrum). The uncharacterized, insoluble yellow solid does not show a ν_{NO} stretching band in the IR (KBr) spectrum.

Photolysis of CH$_2$Cl$_2$ Solutions of [PPN][(NO)Fe(SO$_2$,S-C$_6$H$_4$)(S,S-C$_6$H$_4$)] (4) in the Presence and Absence of PPh$_3$, Respectively.[13] For comparison of photochemical deoxygenation of complex **4** in the presence/absence of triphenylphosphine, the reaction time courses of [O] release (or trapped by 1200 equiv of PPh$_3$) under irradiation in CH$_2$Cl$_2$ at 25 ± 2 °C were studied by monitoring the decay of complex **4** with an intense absorption at 970 nm. The concentration of complex **4** is 1.9 × 10^{-4} M. A 3 mL (concentration 1.9 × 10^{-4} M) of complex **4** was loaded into a septum-sealed UV cell wrapped with aluminum foil in the dark. Then the 1200 equiv of PPh$_3$ (180 mg) was added to the UV cell. The mixture solution was irradiated by Hg lamp (8 W × 8, I_{max} = 417 nm) at 25 ± 2 °C and then monitored immediately by UV−vis. The collected data were analyzed by the Sigmaplot program. Data of the reaction time courses of [O] release in the presence (or absence) of PPh$_3$ were collected in the interval (3 and 5 min, respectively) of the first 75 (100) min. The k_{obs} of the photochemical reaction was conducted under pseudo-first-order conditions. Photolysis of CH$_2$Cl$_2$ solution of complex **4** yielded complex **1** in the presence and absence of PPh$_3$ with k_{obs} = 6.3 × 10^{-4} (R^2 = 0.9987) and 4.8 × 10^{-4} (R^2 = 0.9964) s^{-1} (25 ± 2 °C), respectively. The byproduct Ph$_3$PO was identified by ^{31}P NMR.

Photolysis of CH$_3$CN Solutions of Complex 7 (9).[13] Into a 4 mL quartz reactor was added CH$_3$CN solution (3 mL) of complex **7** (0.1 mM) (or **9**) by syringe, and the reactor was sealed under positive N_2. The solution was irradiated by Hg lamp (8 W × 12, I_{max} = 366 nm) at 20 °C. The reaction was monitored immediately by UV−vis. After 20 min of irradiation, the resulting green-yellow solution had the dominant absorption band at 684 nm, consistent with the formation of complex **10** (670 nm for complex **12**).

Photolysis of CH$_3$CN Solutions of Complex 10.[13] To a 4 mL quartz reactor was added CH$_3$CN solution (3 mL) of complex **10** (0.1 mM) by syringe, and the reactor was sealed under positive N_2. The solution was irradiated by Hg lamp (8 W × 8, I_{max} = 366 nm) at 20 °C, and the reaction was monitored by UV−vis. After 27 min of irradiation, the green-yellow solution shows the electronic absorption of 684 with the same intensity. This result demonstrated the complex **10** is stable under irradiation at 20 °C.

Reaction of Complex 7 and O$_2$. A CH$_3$CN solution (15 mL) of complex **7** (0.051 g, 0.03 mmol) was purged with pure O_2 gas (3.0 mL, 14 psi, at 293 K) by syringe. The flask was tightly sealed, and the reaction solution was stirred at ambient temperature for 72 h. The color of solution gradually turned from yellow-green to brown-purple accompanied by a trace of white solid precipitate. Solvent was removed under vacuum to leave the brown-purple solid. THF (10 mL × 2) was added to extract the purple product, and the solution was transferred to another 50 mL flask. Hexane (15 mL) was then added to precipitate the dark purple solid after the solution was concentrated to 3 mL under vacuum. The dark purple solid was identified as complex **4** (0.023 g, 80%) by UV−vis and IR spectra.

Reaction of Complex 10 and O$_2$. A CH$_3$CN solution (15 mL) of complex **10** (0.148 g, 0.1 mmol) was purged with O_2 (4.0 mL, 14 psi, at 293 K) gas via the syringe, and then the reaction mixture

was allowed to stir for 3 h at room temperature. Rapid change of solution color from green-yellow to red occurred. The solution was concentrated to 3 mL, and diethyl ether (20 mL) was then added to precipitate the red purple solid. After 20 min of standing, solvent was removed by cannula and the red purple solid was dried under vacuum. A solvent mixture of THF−diethyl ether (20:5 mL) was added to extract the dark red product. Recrystallization from THF−hexane diffusion gave dark red crystals of [PPN][(NO)Fe(S,S-$C_6H_4)_2$] (**1**) (0.076 g, 84%) identified by IR and UV−vis spectra. Then, the mixed solvent CH_3CN−THF (5:5 mL) was added to dissolve the remaining residues. Diffusion of diethyl ether into this CH_3CN−THF solution at room temperature for 1 week led to dark purple crystals of $[PPN]_2[Fe(S,S\text{-}C_6H_4)_2]_2$ (0.031 g, 9%) identified by the UV−vis spectrum (λ_{max}: 517, 560, 614 nm), white crystals of $[PPN][NO_3]$ identified by the IR spectrum (υ_{NO}: 1384 cm^{-1} (KBr)), and an unknown product with the PPN^+ cation.

Reaction of Complex 12 and O_2. Complex **12** (0.158 g, 0.1 mmol) was loaded into a 50 mL Schlenk flask, and 5 mL of CH_3CN was added to afford the green-yellow solution. After injection of 30 mL of dry dioxygen gas, the solution was stirred at room temperature for 6 h. The resulting mixture was dried under vacuum, and 10 mL of THF was added. The resulting mixture solution was filtered through a porous filter to separate the insoluble residue and the filtrate. Hexane (20 mL) was added to the filtrate to precipitate the red-brown solid. Diffusion of hexane into the THF solution (3 mL) of the red-brown solid gave red crystals of complex **3** (0.076 g, 72%). The remaining residue was redissolved in CH_2Cl_2 (10 mL) and filtered through Celite. Hexane (30 mL) was then added to precipitate the dark brown solid characterized by X-ray diffraction as the known $[PPN]_2[Fe(S,S\text{-}C_6H_2\text{-}3,6\text{-}Cl_2)_2]_2$ (0.024 g, 11%) and the white $[PPN][NO_3]$ identified by the IR spectrum (ν_{NO}: 1384 cm^{-1} (KBr)).

Magnetic Measurements. The magnetic data were recorded on a SQUID magnetometer (MPMS5 Quantum Design company) under an 1 T external magnetic field in the temperature range 2−300 K. The magnetic susceptibility data were corrected for temperature-independent paramagnetism (TIP, 1×10^{-4} cm^3 mol^{-1}) and ligands' diamagnetism by the tabulated Pascal's constants.

Crystallography. Crystallographic data and structure refinements parameters of complexes **3** and **5**−**12** are summarized in the Supporting Information. Each crystal was mounted on a glass fiber and quickly coated in epoxy resin. Unit-cell parameters were obtained by least-squares refinement. Diffraction measurements for complexes **3** and **5**−**12** were carried out on a SMART CCD (Nonius Kappa CCD) diffractometer with graphite-monochromated Mo Kα radiation ($\lambda = 0.7107$ Å). Least-squares refinement of the positional and anisotropic thermal parameters of all non-hydrogen atoms and fixed hydrogen atoms was based on F^2. A SADABS[25] absorption correction was made. The SHELXTL[26] structure refinement program was employed. In the case of complex **3**, the Cl group is found at disordered positions (Cl(1−4):Cl(1′−4′) = 1/2:1/2), which were refined by partial occupancies. The atoms Fe(1), N(1), O(1), O(2), and O(3) in **7** and Fe(1), N(1), and O(1) in **10** having two sites with equal occupancy factors of 50% were successfully refined, but O(1) in **7** was refined by an isotropic temperature factor. The site occupancy factor of the SO_2 group in complex **12** is 2/3:1/3 (O(2) and O(3):O(2′) and O(3′)) and was refined by partial occupancies.

Acknowledgment. We greatly acknowledge financial support from the National Science Council (Taiwan).

Supporting Information Available: X-ray crystallographic files in CIF format for the structure determinations of $[(NO)Fe(S,SO_2\text{-}C_6H_2Cl_2)(S,S\text{-}C_6H_2\text{-}3,6\text{-}Cl_2)]_2^{2-}$, $[(NO)Fe(S,S\text{-}C_6H_2\text{-}3,6\text{-}Cl_2)_2]^-$, $[(NO)Fe(S,SO_2\text{-}C_6H_3R)(S,S\text{-}C_6H_3R)]^{2-}$ (R = H, *m*-CH_3), $[(NO)Fe(S,SO_2\text{-}C_6H_2Cl_2)(S,S\text{-}C_6H_2\text{-}3,6\text{-}Cl_2)]^{2-}$, $[(NO)Fe(S,S\text{-}C_6H_3R)_2]^{2-}$ (R = H, *m*-CH_3), and $[(NO)Fe(S,S\text{-}C_6H_2\text{-}3,6\text{-}Cl_2)_2]^{2-}$. This material is available free of charge via the Internet at http://pubs.acs.org.

IC050108L

(25) Sheldrick, G. M. *SADABS, Siemens Area Detector Absorption Correction Program*; University of Göttingen: Göttingen, Germany, 1996.
(26) Sheldrick, G. M. *SHELXTL, Program for Crystal Structure Determination*; Siemens Analytical X-ray Instruments Inc.: Madison, WI, 1994.